J. Biochem. 122, 101-108 (1997)

Bound Tris Confounds the Identification of Binding Site Residues in a Paraquat Single Chain Antibody[1]

Mark R. Bowles,*,[2] Terrence D. Mulhern,†,[3] Ross B. Gordon,* Hayley R. Inglis,*,[4] Iain A. Sharpe,*,[5] Jan L. Cogill,* and Susan M. Pond*

*University of Queensland, Department of Medicine, Princess Alexandra Hospital, Ipswich Road, Woolloongabba, Brisbane, QLD, 4102, Australia; and †Biomolecular Research Institute, Melbourne, VIC, 3052, Australia

Received for publication, February 3, 1997

We produced an anti-paraquat single chain antibody (scFv) to investigate its potential use in immunotherapy for paraquat poisoning. However, this scFv was expressed in an insoluble form and only displayed moderate binding affinity. An earlier examination of the pH dependence of antigen binding by the parent paraquat-specific mAb (7D7-3) suggested that the electrostatic effects of a tyrosine residue were important. The aims of the current study were to obtain expression of a soluble scFv (D10) and to increase its binding affinity. The former was achieved by expression in a phagemid vector. Site-directed mutagenesis of tyrosine residues in CDR H3 did not result in improved affinity for paraquat, suggesting that the original pH dependence required re-examination. Nuclear magnetic resonance studies of 7D7-3 Fab revealed that the original observation of the pH-dependent paraquat binding with a mid-point of ~pH 8.9 was due to tightly bound Tris. It appears that as Tris is titrated to a neutral species the energetically unfavourable juxtaposition of its positive charge with that of paraquat is reduced. These findings have broad implications in the interpretation of the pH or salt dependence of any antibody-antigen interaction which should be made cautiously and with regard to the possible interference of buffer components introduced during the preparation of the antibody.

Key words: antibody-antigen interactions, murine antibody, nuclear magnetic resonance, paraquat (1,1′-dimethyl-4,4′-bipyridinium dichloride), pH dependence, single chain antibody, site-directed mutagenesis.

Site-directed mutagenesis has been used to change the binding properties, stability and solubility of antibodies and their fragments on the basis of three-dimensional structural data, electrostatic relationships, and competitive binding experiments (*1-9*). In this investigation we set out to improve the solubility and binding properties of an anti-paraquat single chain (scFv) antibody which is of potential use in immunotherapy for paraquat poisoning (*10, 11*).

Our first anti-paraquat scFv (*12*) was produced from the V_H and V_L variable regions of a murine anti-paraquat mAb 7D7-3 (*13*). These were linked *via* a 15 amino acid $(Gly_4\text{-}Ser)_3$ spacer, chosen to minimise interference with the folding of the V_H and V_L domains (*14*). This scFv was expressed predominantly in an insoluble form by *Escherichia coli* cells and only displayed moderate binding affinity ($K_a = 1.24 \times 10^6\ M^{-1}$) for paraquat (*12*).

To enable us to address both of these problems simultaneously, a commercially available recombinant phage antibody system (RPAS) was used to select anti-paraquat scFv sequences by phage display. Other methods, such as the addition of lysine residues to the linker (*15*) could have been attempted, but the RPAS resulted in expression of soluble scFv in the periplasmic fraction of *E. coli* cells. Site-directed mutagenesis of the third complementarity determining region of the heavy chain (CDR H3) was then used in an attempt to improve the binding characteristics of the soluble scFv. The strategy for site-directed mutagenesis was based on several lines of evidence.

Antibodies that bind haptens, such as paraquat, tend to have binding sites that form a concave pocket (*16*). The distribution of residues used to contact the antigen is not uniform across all CDRs. Three dominate the interactions, namely, L3 (21%), H2 (23%), and H3 (29%) (*17*). Over the last few years, there has been a considerable increase in the number of antibodies for which the structure of the bound and free forms have been determined. This has allowed insight into the variety and magnitude of the conformational changes that can occur upon antigen binding (*18, 19*). The largest individual changes have been observed for CDR H3

[1] Funding for this research was provided by the Lions Kidney and Medical Research Foundation of Queensland and Northern New South Wales, the Australian Government Employees Medical Research Fund and the Australian Mutual Provident Society.

[2] To whom correspondence should be addressed. E-mail: mrb@gpo.pa.uq.edu.au

Present addresses: [3] Oxford Centre for Molecular Sciences, New Chemistry Laboratory, South Parks Road, Oxford OX1 3QT, UK; [4] The Queensland Institute of Medical Research, The Bancroft Centre, Herston Road, Brisbane, QLD, 4006; [5] Centre for Drug Design and Development, University of Queensland, St. Lucia, Brisbane, QLD, 4067.

Abbreviations: Fab, immunoglobulin fragment with antibody binding site; HRP, horseradish peroxidase; PQ-scFV, anti-paraquat single chain antibody; RPAS, recombinant phage antibody system.

which shows the greatest length and sequence variability and, as mentioned, tends to provide the largest proportion of interactions with the antigen. We selected this region as our target.

We had obtained some information about the chemical determinants of the interaction of our paraquat-specific IgG mAb, 7D7-3 (*20*). Because paraquat is a dication at all pH values, electrostatic interactions with negatively charged amino acid residues would be expected. The effect of an amino acid residue titrating with a mid-point of 8.9 was observed in the paraquat-7D7-3 interaction. This titration was ascribed to the involvement of a tyrosine residue at the binding site. This would not be unexpected, because tyrosine has been implicated as the contact residue for several other aromatic haptens (*6, 18, 21-24*). Therefore, we replaced the two tyrosine residues of H3 in our soluble anti-paraquat scFv with glutamic acid residues to increase the putative ionic interaction with paraquat.

In a parallel investigation we used nuclear magnetic resonance to define further the interaction between paraquat and the Fab fragment from which the soluble scFv was derived. Although the original purpose of this study was to facilitate the site-directed mutagenesis, the findings have much broader implications for any antibody directed against small charged species.

MATERIALS AND METHODS

General Materials and Methods—Paraquat, methyl iodide, mercuripapain, dithiothreitol (DTT), iodoacetamide, and pristane were obtained from Sigma Chemical, St Louis, MO. 4,4′-Bipyridyl was obtained from BDH, Poole, UK, and goat anti-rabbit IgG labeled with horseradish peroxidase was obtained from Cappel Worthington Biochemicals, Malvern, PA. [^{13}C]Methyl iodide (99.96%) and deuterated solvents were obtained from Cambridge Isotope Laboratories, Woburn, MA. Restriction endonucleases were obtained from New England Biolabs, Beverley, MA. *Taq* DNA polymerase was obtained from Bresatec, Australia. All other reagents were of analytical grade or higher purity and all solutions were prepared in Milli-Q reagent grade water. Sequencing of double-stranded plasmid DNA was carried out by the Sanger dideoxynucleotide termination procedure (*25*). Unless stated otherwise, molecular biology techniques were based on methods outlined by Sambrook *et al.* (*26*).

Fab and paraquat concentrations were determined spectrophotometrically. A molecular mass of 47,472 Da (based on the 7D7-3 sequence) and a value of 14.0 for $A^{1\%}_{1cm}$ at 280 nm were used for the Fab (*27*). A molar absorption coefficient of 21,100 $M^{-1}\cdot cm^{-1}$ at 256 nm was used for paraquat (*28*).

Cloning the Paraquat scFv Sequence—The commercial Recombinant Phage Antibody System (RPAS) (Pharmacia Biotech) containing the pCANTAB 5E vector was used to obtain an anti-paraquat scFv (PQ-scFv) which was expressed in a soluble form. Plasmid DNA was prepared from clone A24 (*12*) and linearised by digestion at the unique *Xho*I restriction site, upstream of the *pelB* leader sequence. This linearised DNA was used for PCR amplification of the scFv sequence with the murine specific RS primer mix from the RPAS kit under conditions recommended by the manufacturer. The purified *Sfi*I-*Not*I restricted product was cloned into pCANTAB 5E vector and transformed into *E. coli* TG 1 cells.

Expression and Detection of PQ-scFv on Phage Particles—Small-scale cultures of transformed clones were prepared for analysis by ELISA essentially according to the protocols described in the RPAS kit. For the initial screening, individual phagemid clones from the transformation plates were recovered in 96 well v-bottomed microtitre plates (ICN, Costa Mesa, CA) containing 100 μl media/well. Overnight cultures were grown at 37°C and used to inoculate fresh plates. Helper phage (M13K07, Pharmacia Biotech) was added (5×10^7 pfu/well) and the plates were incubated for a further 1 h at 37°C before being centrifuged for 30 min at $1,000\times g$ and the pellets resuspended in 150 μl of media. Phage particles were expressed overnight at 30°C.

Paraquat-specific binding activity determination was carried out on supernatants from these expressions by ELISA using an anti-M13 mAb-horseradish peroxidase (HRP) [EC 1.11.1.7] conjugate (Pharmacia Biotech). The assay was performed according to Johnston *et al.* (*29*) using 5% milk powder in phosphate-buffered saline (PBS) to block non-specific interactions. A competitive ELISA of the supernatants was performed after pre-equilibration (1 h at 37°C) with and without paraquat (200 nM).

Expression and Detection of Soluble PQ-scFv—Plasmid DNA from clones detected by the anti-M13 mAb-HRP ELISA was used to transform *E. coli* HB2151 cells. Recombinant protein was expressed overnight at 30°C after induction with 1 mM isopropyl β-D-thiogalactosidase (IPTG, Progen) and detected using the anti-E tag mAb as recommended by the manufacturer (Pharmacia Biotech). Competitive ELISAs were performed as described for the anti-M13 ELISA to select the clone (D10) with the highest activity.

Site-Directed Mutagenesis—Site-directed mutations were made to the D10 scFv sequence using PCR and the technique of splicing by overlap extension with overlapping sense and antisense primers containing the desired mutation (*30*). The strategy was designed to produce an *Xba*I-*Kpn*I cassette. To create the Y96E, Y96F and Y100iE mutations (numbering according to Kabat *et al.*, *31*), both sense and antisense versions of the primers 5′-CGGTTC**G**-**AG**TCTGGTAAATCCTAT-3′,5′-CGGTTC**TTC**TCTGGT-AAATCCTAT-3′, and 5′-TCTGGTAAATCC**GAA**GCTAT-GGAC-3′, respectively, were used. The altered bases required to achieve the amino acid substitution are shown in bold. These primers were used in conjunction with outside primers, an upstream *Xba*I primer; 5′-TCAGGAA-AGGGTCTAGAGTGGCTG-3′ and a downstream *Kpn*I primer; 5′-TGGTTTCTGCAGGTACCATTCTAA-3′ (restriction sites underlined). The mutant cassette was ligated into clone D10 and transformed into *E. coli* HB2151 cells by electroporation. All mutations were confirmed by DNA sequencing of the 393 bp *Xba*I-*Kpn*I fragment. In addition, a control vector was constructed by making an inframe 522 bp deletion using *Pst*I within the scFv sequence of clone D10. This is predicted to result in the deletion of 174 amino acid residues from the expressed anti-paraquat scFv protein. Such a protein would not be expected to retain any affinity for paraquat. This vector was used to control for any non-specific binding resulting from other proteins expressed from the pCANTAB 5E vector, as well as proteins

derived from the HB 2151 cells. Such non-specific binding was absent. This construct also served as a negative control for non-specific binding of the second antibody in the ELISA.

The Effect of pH on the Binding of Paraquat to scFv and 7D7-3 IgG—For each competitive ELISA, periplasmic extracts of clone D10 and the mutated clones were diluted to yield a linear A_{450} response in 50 mM phosphate buffer ($\mu = 0.15$ with KCl) for the pH range 6-8.5 and in 50 mM carbonate buffer ($\mu = 0.15$ with KCl) for the range pH 9-10. These samples were preincubated with paraquat (0-10^{-4} M) as described above. The binding activities of quadruplicate samples for each concentration of paraquat were determined essentially as described for the phage particles with the replacement of the anti-M13 mAb-HRP conjugate by anti-E-tag HRP antibody. E-tag is a peptide tag located at the carboxyl terminus of scFv expressed using the pCANTAB 5E vector. As a control, the periplasmic extract of D10 was assayed on each plate. The concentration of paraquat that reduced the binding activity to 50% of the maximum value, the IC_{50}, was determined by iterative sigmoidal curve fitting using the InPlot program (GraphPad Software, San Diego, CA). Relative affinity was determined by comparing the IC_{50} values as described by Rath *et al.* (*32*). Only the relative affinities may be determined by this method.

7D7-3 IgG (γ2b, κ) was purified from hybridoma culture supernatant by Protein A Sepharose chromatography using a HiTrap Affinity column (Pharmacia Biotech) according to the manufacturer's instructions with the exception that phosphate buffer (50 mM, pH 8.0) was used as the neutralising buffer to avoid Tris contamination. Association constants for IgG-paraquat binding were determined between pH 6.0 and 9.5 by competitive ELISAs (*20*). These assays, which measure the unbound IgG after pre-equilibration of IgG and PQ, result in determination of a valid thermodynamic association constant.

Purification of Recombinant PQ-scFv—The periplasmic extract was isolated and the scFv purified by anion exchange HPLC on Fractogel EMD DEAE-650(M) (Waters, Milford, MA). Buffer A consisted of 20 mM Tris HCl, pH 8.0, and buffer B consisted of 20 mM Tris-HCl, pH 8.0, 0.5 M NaCl. Samples were eluted using a stepwise gradient to 100% buffer B over 80 min. The flow rate was 1.0 ml/min. The purity of the peak containing paraquat-binding activity (measured in an anti-E tag ELISA) was assessed by SDS-PAGE and analytical HPLC gel filtration on a Protein-Pak 2000SW column (Waters).

Fab Preparation—The 7D7-3 hybridoma cell line was amplified in murine ascites and the resultant IgG was purified and papain-digested to produce Fab fragments as described previously (*10*). Fab isoforms were separated by anion exchange HPLC on Fractogel EMD DEAE-650(M). Buffer A consisted of 15 mM Tris-HCl, pH 9.0, and buffer B consisted of 15 mM Tris-HCl, pH 9.0, with 0.5 M NaCl. Samples were eluted for 100 min with buffer A followed by a linear gradient to 25% buffer B over another 100 min. The flow rate was 1.0 ml/min. The purity of the peak was assessed by IEF on Ampholine PAGplate precast gels (LKB, Uppsala, Sweden). The bulk of 7D7-3 Fab (~67%) was a single isoform (pI = 8.3). It was this material that was prepared on a large scale and used in the NMR experiments.

General NMR Techniques—NMR experiments were performed on Bruker AMX-500 and AMX-600 spectrometers. Two-dimensional (2D) spectra were recorded in the phase-sensitive mode using time-proportional phase incrementation (*33*). Spectra were processed using UXNMR (Bruker) and analysed using FELIX (version 2.05, Biosym).

The pH of NMR samples was adjusted with small additions of 0.1 M NaO^2H or ^2HCl. Reported pH values are at room temperature and uncorrected for deuterium isotope effects. The ^1H chemical shifts were referenced either directly to internal 2,2-dimethyl-2-silapentane-5-sulfonate (DSS) (0.0 ppm), or indirectly *via* the residual H_2O signal. The ^{13}C chemical shifts were referenced directly to internal dioxane at 69.4 ppm or DSS at 0.15 ppm (*34*). Where no internal reference was used, ^{13}C chemical shifts were referenced *via* the absolute frequency of 0 ppm for ^1H, using a ratio of $^{13}C/^1H$ of 0.25144952 (*35*).

Synthesis of [^{13}C]Paraquat—Paraquat labeled with ^{13}C at both methyl carbons was produced by the reaction of [^{13}C]methyl iodide with 4,4′-bipyridine in dry chloroform. The reaction mixture was stirred at room temperature for a period of 7 days. Assay by HPLC (*36*) showed this material to be >99% paraquat. [^{13}C]Paraquat purity was confirmed by NMR in that it had essentially identical ^1H and ^{13}C chemical shifts to non-isotopically enriched paraquat and the methyl ^1H signal was a doublet with $^1J_{C\text{-}H} = 146$ Hz.

NMR Experiments on 7D7-3 Fab—Fab samples for NMR experiments were prepared by dissolving lyophilised protein in 99.96% ^2H_2O. Two-dimensional ^{13}C heteronuclear multiple-quantum coherence (HMQC) spectra were recorded with a $1/2J_{C\text{-}H}$ delay of 3.4 ms, 50 t_1 increments, 320 scans/increment and a recycle time (defined here as the time between the start of data acquisition and the beginning of the next pulse train) of 5.3 s (*37*). Two-dimensional ^{13}C heteronuclear multiple-bond coherence (HMBC) spectra were recorded with a $1/2J_{C\text{-}H}$ delay of 125 ms, 50 t_1 increments, 320 scans/increment and a recycle time of 10.3 s (*38*). ^1H longitudinal (T_1) relaxation rates were measured using inversion recovery experiments (*39*).

NMR Line-Width Measurements—^1H NMR line-widths were measured for bound paraquat from the 2D HMQC spectrum of [^{13}C]paraquat in the presence of Fab at paraquat: Fab ratios of approximately 2:1 and 10:1. The bound and free signals were located, then the ^{13}C sweep width (ω_1) was set to 5 ppm to improve the digital resolution in this dimension.

The 2D data were processed as a 2K × 2K matrix without the application of any window function in either dimension. The ω_2 rows corresponding to the maxima of the crosspeaks were extracted, inverse Fourier-transformed and zero filled to 64 K complex data points. The FID was Fourier transformed with no window function and the line-widths measured at half height. To improve the signal-to-noise ratios for weak peaks, exponential window functions with line broadenings ranging from 0.5 to 5.0 Hz were applied prior to Fourier transformation. The line-widths obtained after taking the line broadening into account agreed well with the line-widths without line-broadening.

RESULTS

DNA Sequence of PQ-scFv Clones—The nucleotide sequence for the scFv of clone D10 was different from that of its parent clone (A24) at the 5′- and 3′-termini. This result is not unexpected as primers with degenerate coding were utilised for the PCR amplification of the scFv sequence from A24. In D10, the sequence (ATGGCC) originating from the tail of the *pel*B signal sequence of A24 predicts the addition of methionine and alanine to the start of the V_H domain. In addition, the first codon (GAG) of the scFv sequence from clone A24 has been changed to CAG in D10, resulting in the substitution of glutamic acid by a glutamine residue. At the carboxy terminus of D10, the 3′ degenerate PCR primers have resulted in a change of the second last amino acid residue of the V_L domain from an isoleucine (ATC) to a leucine (CTG). The stop codon has been changed to a codon (CGG) which predicts an arginine residue. No other sequence differences were observed.

Electrophoretic Analysis—No prominent band of expressed recombinant protein was observed on SDS-PAGE of the periplasmic extract from *E. coli* HB 2151 cells containing clone D10. However, on Western blotting and visualisation using an anti-E tag antibody HRP conjugate, two bands were observed at positions corresponding to 31 kDa and 62 kDa (results not shown). The size of the scFv fused to the E tag (18 amino acids) was calculated from the predicted amino acid sequence to be 31.0 kDa.

Expression of the Y100iE mutant was observed only in samples of the whole cell extracts (results not shown); expression in the periplasm was insufficient to assess relative affinity for paraquat by competitive ELISA. This unexpectedly meagre expression into the periplasm was found consistently with other clones from the Y100iE mutagenesis. Sequencing of the 393 bp *Xba*I/*Kpn*I cassette of the CDR H3 revealed the Y100iE mutation but no additional ones. In order to check for the presence of unknown mutations elsewhere in clone Y100iE which might be contributing to the poor expression, the *Xba*I/*Kpn*I cassette from the normal D10 clone was exchanged into Y100iE. Expression was restored, indicating that the property of poor expression was associated with the cassette containing the Y100iE mutation.

Purification of PQ-scFv—Paraquat-binding activity was resolved into a single protein peak by anion exchange chromatography. SDS-PAGE and analytical gel filtration (Fig. 1) demonstrated that this peak was ~90% pure and present as a mixture of monomer (31 kDa) and dimer (62 kDa). Both monomer and dimer exhibited paraquat-binding activity. The yield of scFv was 0.57 mg/liter of induced culture. Analysis of the SDS-PAGE gel by laser scanning densitometry (Molecular Dynamics, Sunnyvale, CA) showed that the scFv was present as 59% dimer and 31% monomer (see inset Fig. 1), whereas an estimated 88% dimer and 2% monomer was obtained by gel filtration. The reason for this discrepancy is the denaturing effect of SDS, which separates non-covalently linked dimers. Similar dimerisation has been reported for another PQ-scFv (*40*).

Effect of pH on Binding Affinity—The effect of pH on IC_{50} values for D10, and its Y96E and Y96F mutants is shown in Fig. 2. While at some pH values there was a significant difference between D10 and the Y96F mutant, there was only a ~3-fold difference in the IC_{50} values across the entire pH range. There was no clear trend in the effect of pH on binding affinity. The IC_{50} value at pH 7.4 for the parent mAb 7D7-3 calculated using the association constant and a concentration equal to that of the D10 is 5.7×10^{-9} M.

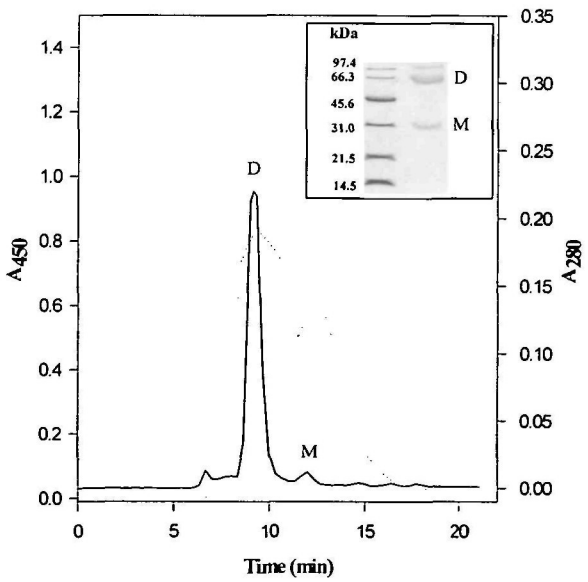

Fig. 1. **Molecular size exclusion and SDS-PAGE analysis of PQ-scFv.** The solid line (—) shows the A_{280} of the eluate from analytical HPLC gel filtration on a Protein-Pak 2000SW column at a flow rate of 1 ml/min in 50 mM phosphate buffer, pH 7.4. The ELISA activity towards paraquat is shown by the dotted line (·····), which reflects the A_{450}. An SDS-PAGE analysis using a 12% polyacrylamide gel performed according to Sambrook *et al.* (1989) is shown in the inset. The sample buffer for this analysis contained 5% (v/v) 2-mercaptoethanol. The monomer and dimer of PQ-scFv are shown by M and D, respectively.

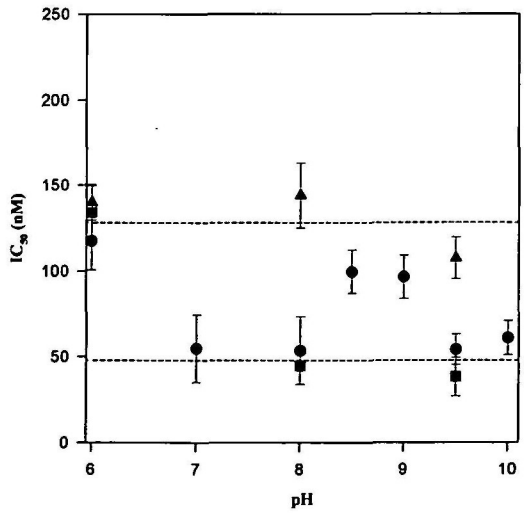

Fig. 2. **The effect of pH on the binding of PQ-scFv and its mutants to paraquat.** IC_{50} values (±1 standard deviation) are shown for the parent PQ-scFv (D10, ●), and its mutants Y96F (■), and Y96E (▲). Error bars indicate two standard errors. The dashed lines (····) indicate the extremes of the deviation (two standard errors) associated with an average of all of the IC_{50} values for D10 and the two mutants.

This value is about one order of magnitude lower than the equivalent value for D10, consistent with previous comparisons (*15*).

In contrast to 7D7-3 IgG purified in the presence of Tris-HCl buffer (*20*), no pH dependence for the binding of paraquat to IgG was exhibited in this study (Fig. 3). The average value of the association constant for the Tris-free purification was $2.18 \pm 1.23 \times 10^8\ M^{-1}$ compared with $2.15 \times 10^8\ M^{-1}$ calculated for the high pH plateau shown in Fig. 3 by Bowles and Pond (*20*).

NMR Studies of Free Paraquat—The 2,6 and 3,5 ^{13}C resonances were assigned from a HMQC experiment at natural abundance. The ^1H and ^{13}C chemical shifts of free paraquat were found to be independent of both temperature (278-298 K) and pH (7.1-10.6) in aqueous solution and are listed in Table I. The T_1 relaxation times for free paraquat were measured from inverse recovery experiments in H_2O and ^2H_2O at 298 K. The T_1 value for the methyl protons was 1.45 s in H_2O and 1.48 s in ^2H_2O. For the 2,6 ring protons T_1 was 2.98 s in H_2O and 3.07 s in ^2H_2O and for the 3,5 protons it was 2.89 s in H_2O and 3.08 s in ^2H_2O.

The Interaction of Paraquat and Fab—The ^1H NMR spectrum of the Fab in ^2H_2O in the absence and presence of paraquat showed loss of some protein resonances and appearance of new protein resonances as aliquots (0-2 mol equivalents) of paraquat were added to the Fab up to a ratio of 2:1 of paraquat:Fab.

The intrinsic broadness of the bound paraquat signals ($\nu_{1/2} \sim 25$ Hz) and extensive overlap with the Fab resonances mean that bound paraquat resonances could only be detected in experiments involving the ^{13}C-labeled paraquat. HMQC and HMBC experiments were used to assign free and bound resonances (see Table I). Although paraquat itself has twofold symmetry relating the two pyridyl ring systems (chemically and magnetically equivalent primed and non-primed positions), separate resonances were observed for the 7 and 7′ methyl groups. The magnetic environment of the binding site must, therefore, be asymmetric. This is not surprising, as the antibodies were raised against the paraquat hapten secured by an alkyl linker to a protein carrier (*13*) resulting in antibodies tailored to bind this asymmetric paraquat derivative. As a result, the antibody would not be expected to bind both methyl groups equivalently.

Interaction of Tris with 7D7-3 Fab—Several sharp impurity peaks were observed in the NMR spectrum of 7D7-3 Fab. A sharp singlet at 3.72 ppm, displayed a pH-dependent chemical shift and on the basis of this pH dependency was identified as Tris. Tris buffers were used extensively throughout the Fab purification. From an analysis of the integrated intensity of the Tris signal 1-2 mol equivalents of Tris to Fab are present. The variation with pH of the ^1H chemical shift of the methylene protons in Tris in ^2H_2O at 298 K reflects a pK_a' of 8.34. The manufacturer reports the pK_a' of Tris in H_2O at 298 K is 8.1.

The ^1H NMR spectra of solutions containing 1.0 mM Tris

TABLE I. **The ^{13}C and ^1H chemical shifts (δ) for paraquat in the presence and absence of 7D73 Fab.** Spectra of free paraquat were recorded at 298, 288, 283, and 278 K (pH 7.1). Chemical shifts for paraquat in the paraquat-Fab complex were measured from HMQC spectra recorded in aqueous solutions containing 0.07 mM Fab and 0.14 mM or 0.7 mM ^{13}C-enriched (7,7′ positions) paraquat at 298 K (pH 7.15). The variation in chemical shift determinations varied by less than 0.02 ppm for ^1H and by less than 0.06 ppm for ^{13}C.

Position	$\delta^{13}C$ (ppm)	$\delta^{13}C$ (ppm) bound	δ^1H (ppm)	δ^1H (ppm) bound	$^1J_{C\text{-}H}$ (Hz)
7	51.2	49.5	4.50	3.65	146
7′	51.2	51.4	4.50	4.06	
2,6	149.1		9.05		176
3,5	129.5		8.52		192
4	152.6		–		–

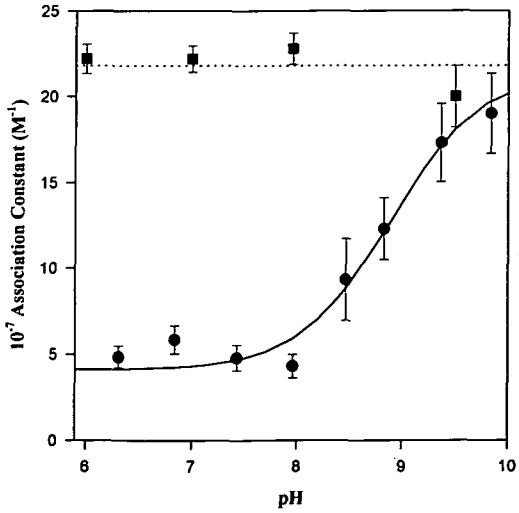

Fig. 3. **Association constant-pH profiles for the interaction of paraquat and 7D73 IgG.** Experimental data are shown for IgG purified in the presence of Tris buffer (●) and in its absence (■). The solid line is based on a pK_a' of 8.9 and limiting values for the association constant of 4.1×10^7 and $21.5 \times 10^7\ M^{-1}$, at low and high pH, respectively. The dashed line (····) is the mean of the association constants obtained with IgG purified in the absence of Tris. All error bars indicate 1 standard deviation.

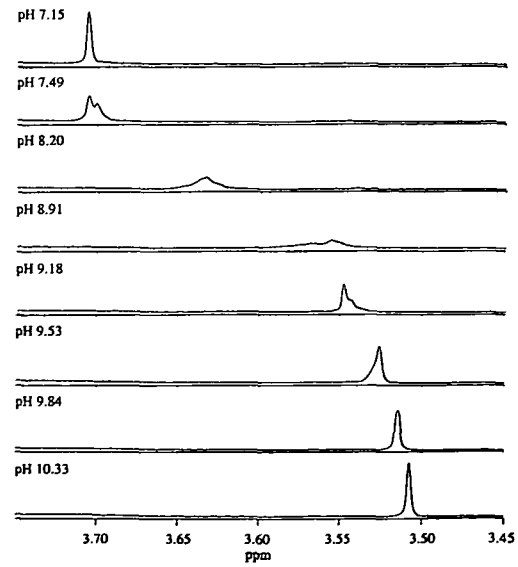

Fig. 4. **NMR titration of the Tris signal in 7D73 Fab in the presence of paraquat.** Expansions of ^1H NMR spectra recorded on a sample of 70 mM Fab with 0.14 mM paraquat in ^2H_2O at 298 K.

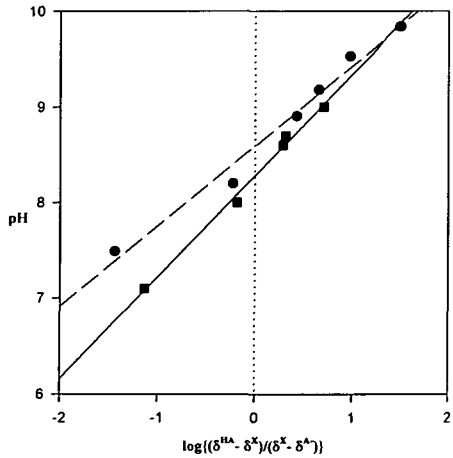

Fig. 5. **Determination of the pK_a' of Tris in the absence and presence of 7D73 Fab.** Limiting values for the chemical shift of the Tris signal of 3.70 ppm at low pH (δ^{HA}) and 3.51 ppm at high pH (δ^{A-}) have been used in a modified version of the Henderson-Hasselbach equation on data generated in the absence (■) and presence (●) of 7D73 Fab. The intercepts of the linear regressions yield the pK_a' of Tris in the absence (8.3) and presence (8.6) of 7D73 Fab. All measurements were made at 298 K in ^2H_2O.

and varying concentrations of paraquat were recorded at different pH values. The line-shape and pH dependency of the chemical shift of the Tris signals were unaffected by the amount of paraquat. The ^1H NMR spectrum of Fab (with the Tris contaminant) was recorded at pH values from 7 to 10.5. The Tris peak displayed the same chemical shift pH dependence as free Tris and the signal was sharp ($\nu_{1/2} = 1.9 \pm 0.6$ Hz). However, in the presence of 7D7-3 Fab and paraquat, the line-shape of Tris signal was modulated by the pH of the solution (Fig. 4). This suggests that Tris only binds to paraquat in a ternary complex and that the binding interaction is dependent on the ionisation state of both Tris and the paraquat-Fab complex. The pK_a' determined from the mid-points of the broadened Tris signals was 8.60 (Fig. 5).

DISCUSSION

The aims of the present study were to obtain expression of a soluble scFv and to increase its binding affinity by mutagenesis of the CDR H3. After PCR amplification of the scFv sequence from a parent clone (A24), transfer into the commercial pCANTAB 5E vector and phage selection, we achieved soluble scFv expression at levels which were comparable with those reported previously. The clone with the highest affinity for paraquat (D10) showed minor differences in the N- and C-terminal sequences of the V_H region from the clone A24. These resulted from the use of degenerate primers in the PCR and may have contributed to the increased solubility. The expression vector for clone A24 (pPOW) contained the extremely strong λ left and right promoters, cloned in tandem for high-level production of antibody fragments (*41*). High expression of heterologous proteins into the periplasmic space overloads the host's transport and folding machinery, as demonstrated by the gradual accumulation of non-functional and probably incorrectly folded protein (*42*).

Site-directed mutagenesis was used to change the two tyrosine residues at positions 96 and 100i to glutamic acid residues. This did not result in improved affinity for paraquat. Results from the Y96E mutation imply that the electrostatic interactions provided by the glutamic acid residue do not substantially alter paraquat binding. The similar affinities of the Y96E, Y96F, and D10 suggest that Y96 is not involved in paraquat binding. Neither the mutants nor the D10 scFv exhibited the pH dependence shown previously by the parent IgG (*20*).

There was no detectable expression of Y100iE into the periplasm. Neither mutation of the gene III signal sequence nor the introduction of positive charges downstream from this sequence can be invoked to explain the lack of expression into the periplasm (*43*). The profound effect of mutating the 100i residue on expression of this scFv to a glutamic acid residue cannot be explained by the available data.

The NMR analysis of the Fab revealed that Tris was present despite exhaustive dialysis against water, lyophilisation and reconstitution in ^2H_2O. Close inspection of the Tris signal in solutions containing Fab and paraquat indicates that as the pH is increased above 7 the Tris signal splits into at least two resonances. Then broadening occurs, with a maximum line-width ($\nu_{1/2} \sim 18$ Hz) at around pH 9. Thereafter, the signals begin to coalesce and sharpen until, at pH values > 10, only a sharp singlet is present (Fig. 4). This pH-dependent splitting and broadening of the Tris signal does not occur in solutions containing Tris plus paraquat alone or in solutions containing Tris plus Fab alone. It only occurs when Tris, Fab, and paraquat are present at the same time and then only within a relatively narrow pH window, between pH$\sim$7.3 and $\sim$9.5.

The broadening (indicative of a binding interaction) followed by sharpening of the signal (as the pH is raised) seems consistent with an interaction between the charged form of Tris and an ionised form of the paraquat-Fab complex. The pI of the 7D7-3 Fab fragment is 8.3, which is similar to the pK_a' of Tris. However, the broadening behaviour does not seem to be symmetrical about this pH but rather about the pK_a' of Tris in the ternary complex, which is $\sim$8.6. Furthermore, the fact that the Tris signal is no longer broadened at high pH suggests that only the positively charged form of Tris interacts with an ionised form of the paraquat-Fab complex. Upon re-examination of the parent IgG, purified in the absence of Tris, no pH-dependent binding affinity was observed. Similarly, neither the mutants, nor the D10 scFv exhibited the pH dependence shown previously by the parent IgG (*20*). These results suggest that the original observation of a pH dependence for paraquat binding with a mid-point of $\sim$pH 8.9 in this system was due to tightly bound Tris. It appears that as Tris is titrated to a neutral species there is a reduction in the energetically unfavourable juxtaposition of its positive charge with that of paraquat.

The presence of Tris at the antibody binding site would not have been revealed without NMR analysis. The implications of the binding of such a buffer component extend beyond the paraquat-antibody system to all interactions of binding proteins that bind charged species. The results have obvious implications for investigations of the antibody interactions with haptens such as phosphorylcholine (*4, 23, 44-47*). The possible effects of tightly bound buffer compo-

nents are not limited to haptens but would influence electrostatic interactions between larger antigens and their antibodies. Interpretation of the pH or salt dependence of an antibody-antigen interaction should be made cautiously and with regard to the possible interference of buffer components introduced during the preparation of the antibody.

TDM was in receipt of an Australian Post-Graduate Award. The authors thank Dr. Ray Norton for his assistance in carrying out the NMR experiments.

REFERENCES

1. Sharon, J., Gefter, M.L., Manser, T., and Ptashne, M. (1986) Site-directed mutagenesis of an invariant amino acid residue at the variable-diversity segments junction of an antibody. *Proc. Natl. Acad. Sci. USA* **83**, 2628-2631
2. Roberts, S., Cheetham, J.C., and Rees, A.R. (1987) Generation of an antibody with enhanced affinity and specificity for its antigen by protein engineering. *Nature* **328**, 731-734
3. Panka, D.J., Very, D.L., Jacobson, B.A., Kussie, P.H., Parhami, S.B., Margolies, M.N., and Marshak-Rothstein, A. (1993) Defining the structural correlates responsible for loss of arsonate affinity in an IDCR antibody isolated from an autoimmune mouse. *Mol. Immunol.* **30**, 1013-1020
4. Kussie, P.H., Parhami, S.B., Wysocki, L.J., and Margolies, M.N. (1994) A single engineered amino acid substitution changes antibody fine specificity. *J. Immunol.* **152**, 146-152
5. Schildbach, J.F., Near, R.I., Bruccoleri, R.E., Haber, E., Jeffrey, P.D., Ng, S.C., Novotny, J., Sheriff, S., and Margolies, M.N. (1993) Heavy chain position 50 is a determinant of affinity and specificity for the anti-digoxin antibody 26-10. *J. Biol. Chem.* **268**, 21739-21747
6. Martinez-Yamout, M. and McConnell, H.M. (1994) Site-directed mutagenesis and ^{1}H nuclear magnetic resonance of an anti-dinitrophenyl spin label antibody. *J. Mol. Biol.* **244**, 301-318
7. Young, N.M., MacKenzie, C.R., Narang, S.A., Oomen, R.P., and Baenziger, J.E. (1995) Thermal stabilization of a single-chain Fv antibody fragment by introduction of a disulphide bond. *FEBS Lett.* **377**, 135-139
8. Benhar, I. and Pastan, I. (1995) Identification of residues that stabilize the single-chain Fv of monoclonal antibodies B3. *J. Biol. Chem.* **270**, 23373-23380
9. Knappik, A. and Pluckthun, A. (1995) Engineered turns of a recombinant antibody improve its in vivo folding. *Protein Eng.* **8**, 81-89
10. Chen, N.C., Bowles, M.R., and Pond, S.M. (1994) Prevention of paraquat toxicity in suspensions of alveolar type II cells by paraquat-specific antibodies. *Hum. Exp. Toxicol.* **13**, 551-557
11. Nagao, M. (1989) Production and toxicological application of anti-paraquat antibodies. *Nippon Hoigaku Zasshi* **43**, 134-147
12. Devlin, C.M., Bowles, M.R., Gordon, R.B., and Pond, S.M. (1995) Production of a paraquat specific murine single chain Fv fragment. *J. Biochem.* **118**, 480-487
13. Bowles, M.R., Johnston, S.C., Schoof D.D., Pentel, P.R., and Pond, S.M. (1988) Large scale production and purification of paraquat and desipramine monoclonal antibodies and their Fab fragments. *Int. J. Immunopharmacol.* **10**, 537-545
14. Huston, J.S., McCartney, J., Tai, M.S., Mootola-Hartshorn, C., Jin, D., Warren, F., Keck, P., and Oppermann, H. (1993) Medical applications of single-chain antibodies. *Int. Rev. Immunol.* **10**, 195-217
15. Bird, R.E., Hardman, K.D., Jacobson, J.W., Johnson, S., Kaufman, B.M., Lee, S.M., Lee, T., Pope, S.H., Riordan, G.S., and Whitlow, M. (1988) Single-chain antigen-binding proteins. *Science* **242**, 423-426 and *erratum* in *Science* (1989) **244**, 409
16. Rini, J.M., Schultz-Gahmen, U., and Wilson, I.A. (1992) Structural evidence for induced fit mechanism for antibody-antigen recognition. *Science* **255**, 959-965
17. Wilson, I.A. and Stanfield, R.L. (1994) Antibody-antigen interactions: new structures and new conformational changes. *Curr. Opin. Struc. Biol.* **4**, 857-867
18. Stanfield, R.L., Takimoto-Kamimura, M., Rini, J.M., Profy, A. T., and Wilson, I.A. (1992) Major antigen-induced domain rearrangements in an antibody. *Structure* **1**, 83-93
19. Wu, T.T., Johnson, G., and Kabat, E.A. (1992) Length distribution in CDRH3 in antibodies. *Proteins* **16**, 1-7
20. Bowles, M.R. and Pond, S.M. (1990) The importance of electrostatic interactions in the binding of paraquat to its elicited monoclonal antibody. *Mol. Immunol.* **27**, 847-852
21. Takahashi, H., Odaka, A., Kawaminami, S., Matsunaga, C., Kato, K., Shimada, I., and Arata, Y. (1991) Multinuclear NMR study of the structure of the Fv fragment of anti-dansyl mouse IgG2a antibody. *Biochemistry* **30**, 6611-6619
22. McManus, S. and Reichmann, L. (1991) Use of 2D NMR, protein engineering and molecular modelling to study the hapten-binding site of an antibody Fv fragment against 2-phenyloxazolone. *Biochemistry* **30**, 5851-5857
23. Omelyanenko, V.G., Jiskoot, W., and Herron, J.N. (1993) Role of electrostatic interactions in the binding of fluorescein by anti-fluorescein antibody 4-4-20. *Biochemistry* **32**, 10423-10429
24. Odaka, A., Kim, J.I., Takahashi, H., Shimada, I., and Arata, Y. (1992) Isotope-edited nuclear magnetic resonance study of Fv fragment of anti-dansyl mouse monoclonal antibody: recognition of the dansyl hapten. *Biochemistry* **31**, 10686-10691
25. Kraft, R., Tardiff, J., Krauter, K.S., and Leinwand, L.A. (1988) Using mini-prep plasmid DNA for sequencing double stranded templates with Sequenase. *BioTechniques.* **6**, 544-546
26. Sambrook, J., Fritsch, E.F., and Maniatis, T. (1989) *Molecular Cloning: A Laboratory Manual*, 2nd ed., Cold Spring Harbor Laboratory Press, Cold Spring Harbor, NY
27. Eisen, H.N., Simms, E.S., and Potter, M. (1968) Mouse myeloma proteins with antihapten antibody acitivity. The protein produced by plasma cell tumor MOPC-315. *Biochemistry* **7**, 4126-4134
28. Verhoeven, J.W., Verhoeven-Schoff, A.-M., Masson, A., and Schwyzer, R. (1974) The use of paraquat as an NMR and charge transfer probe for solvent-exposed aromatic amino acid side chains. *Helv. Chim. Acta* **57**, 2503-2514
29. Johnston, S.C., Bowles, M.R., Winzor, D.J., and Pond, S.M. (1988) Comparison of paraquat-specific murine monoclonal antibodies produced by *in vitro* immunization. *Fund. Appl. Toxicol.* **11**, 261-267
30. Ho, S.N., Hunt, H.D., Horton, R.M., Pullen, J.K., and Pease, L.R. (1989) Site-directed mutagenesis by overlap extension using the polymerase chain reaction. *Gene* **77**, 51-59
31. Kabat, E.A., Wu, T.T., Perry, H.M., Gottesman, K.S., and Foeller, C. (1991) Sequences of Proteins of Immunological Interest. U.S. Department of Health and Human Services, Public Health Service, NIH, NIH Publication No. 91-3242, Bethesda, MD
32. Rath, S., Stanley, C.M., and Steward, M.W. (1988) An inhibition enzyme immunoassay for estimating relative antibody affinity and affinity heterogeneity. *J. Immunol. Methods* **106**, 245-249
33. Marion, D. and Wuthrich, K. (1983) Application of phase sensitive two-dimensional correlated spectroscopy (COSY) for measurements of ^{1}H-^{1}H spin-spin coupling constants in proteins. *Biochem. Biophys. Res. Commun.* **113**, 967-974
34. Wishart, D.S. and Sykes, B.D. (1994) The ^{13}C chemical-shift index: a simple method for the identification of protein secondary structure using ^{13}C chemical-shift data. *J. Biomol. NMR* **4**, 171-180
35. Bax, A.D. and Subramanian, S. (1986) Sensitivity-enhanced two-dimensional heteronuclear shift correlation NMR spectroscopy. *J. Magn. Reson.* **67**, 565-569
36. Gill, R., Qua, S.C., and Moffat, A.C. (1983) High-performance liquid chromatography of paraquat and diquat in urine with rapid sample preparation involving ion-pair extraction on disposable cartridges of octadecyl-silica. *J. Chromatogr.* **255**, 483-490
37. Bax, A.D., Griffey R.H., and Hawkins, B.L. (1983) Correlation of proton and Nitrogen-15 chemical shifts by multiple quantum NMR. *J. Magn. Reson.* **55**, 301-305

38. Bax, A.D. and Summers, M.F. (1986) ^{1}H and ^{13}C assignments from sensitivity-enhanced detection of heteronuclear multiple-bond connectivity by 2D multiple quantum NMR. *J. Am. Chem. Soc.* **108**, 2093-2094
39. Vold, R.L., Waugh, J.S., Klein, M.P., and Phelps, D.E. (1968) Measurement of spin relaxation in a complex system. *J. Chem. Phys.* **48**, 3831-3832
40. Graham, B.M., Porter, A.J.R., and Harris, W.J. (1995) Cloning, expression and characterisation of a single chain antibody fragment to the herbicide paraquat. *J. Chem. Tech. Biotechnol.* **63**, 279-289
41. Power, B.E., Ivancic, N., Harley, V.R., Webster, R.G., Kortt, A.A., Irving, R.A., and Hudson, P.J. (1992) High-level temperature-induced synthesis of an antibody V_H-domain in *Escherichia coli* using the Pel B secretion signal. *Gene* **113**, 95-99
42. Lilley, G.G., Dolezal, O., Hillyard, C.J., Bernard, C., and Hudson, P.J. (1994) Recombinant single-chain antibody peptide conjugates expressed in *Escherichia coli* for the rapid diagnosis of HIV. *J. Immunol. Methods* **171**, 211-226
43. Larrick, J.W. (1995) Variable region sequence modulates periplasmic export of a single-chain Fv antibody fragment in *Escherichia coli*. *BioTechniques* **18**, 832-841
44. Jackson, D.Y., Prudent, J.R., Baldwin, E.P., and Schultz, P.G. (1991) A mutagenesis study of a catalytic antibody. *Proc. Natl. Acad. Sci. USA* **88**, 58-62
45. Kang, A.S., Barbas, C.F., Janda, K.D., Benkovic, S.J., and Lerner, R.A. (1991) Linkage of recognition and replication functions by assembling combinatorial antibody Fab libraries along phage surfaces. *Proc. Natl. Acad. Sci. USA* **88**, 4363-4386
46. Anchin, J.M., Droupadi, P.R., DuBois, G.E., Kellogg, M.S, Nagarajan, S., Carter, J.S., and Linthicum, D.S. (1994) Identification of residues in monoclonal antibody NC10.8 that bind to the sweetener *N*-(*p*-cyanophenyl)-*N'*-(diphenylmethyl)guanidinoacetic acid by using radioligand binding, absorption and fluorescence spectroscopy, computer-aided molecular modeling, and site-directed mutagenesis. *J. Immunol.* **153**, 3059-3069
47. Parhami, S.B., Kussie, P.H., Strong, R.K., and Margolies, M.N. (1993) Conservation of binding site geometry among *p*-azophenylarsonate-specific antibodies. *J. Immunol.* **150**, 1829-1837